Semicond. Sci. Technol. **23** (2008) 035006 (6pp) doi:10.1088/0268-1242/23/3/035006

Temperature-dependent behavior of Ti/p-InP/ZnAu Schottky barrier diodes

Sezai Asubay[1], Ömer Güllü[2], Bahattin Abay[2], Abdulmecit Türüt[2] and Ali Yilmaz[1]

[1] University of Dicle, Faculty of Science & Art, Department of Physics, Diyarbakır, Turkey
[2] Atatürk University, Faculty of Sciences and Arts, Department of Physics, 25240 Erzurum, Turkey

Received 2 October 2007, in final form 19 December 2007
Published 31 January 2008
Online at stacks.iop.org/SST/23/035006

Abstract

The current–voltage (I–V) characteristics of Ti/p-InP Schottky diodes have been measured in a wide temperature range with a temperature step of 20 K. An experimental barrier height (BH) Φ_{ap} value of about 0.85 eV was obtained for the Ti/p-InP Schottky diode at 300 K. A decrease in the experimental BH Φ_{ap} and an increase in the ideality factor n with a decrease in temperature have been explained on the basis of a thermionic emission mechanism with the Gaussian distribution of the barrier heights due to the BH inhomogeneities at the metal–semiconductor interface. $\bar{\Phi}_b$ and A^* as 1.01 eV, and 138 A cm^{-2} K^2, respectively, have been calculated from a modified $\ln(I_0/T^2) - q^2\sigma_s^2/2k^2T^2$ versus $1/T$ plot. This BH value is in close agreement with the values of 0.99 eV obtained from the Φ_{ap} versus $1/T$ and $\ln(I_0/T^2)$ versus $1/n$T plots.

(Some figures in this article are in colour only in the electronic version)

1. Introduction

Schottky barrier diodes (SBDs) are simplest of metal–semiconductor (MS) contact devices due to their technological importance [1–5]. In particular, the SBDs have important applications in bipolar integrated circuits such as clamps, load resistor, couplers and level shifters [5–8]. Moreover, the SBDs play an important role in devices operating at cryogenic temperatures as infrared detectors, sensors in thermal imaging, microwave diodes, gates of transistors and infrared and nuclear particle detectors [8–14]. Therefore, analysis of the current voltage (I–V) characteristics of the SBDs at room temperature does not only give detailed information about their conduction process or the nature of barrier formation at the MS interface [5–19]. The temperature dependence of the I–V characteristics allows us to understand different aspects of conduction mechanisms [19–39].

In the present study, Ti Schottky contacts on a p-InP substrate were formed, and the I–V characteristics of the obtained Ti/p-InP/Ni Schottky diodes were measured in a wide temperature range with a temperature step of 20 K. The temperature-dependent barrier characteristics of the diodes have been interpreted on the basis of a thermionic emission mechanism with a Gaussian spatial distribution of barrier heights around a mean value due to barrier height inhomogeneities prevailing at the MS interface, and the Richardson constant of the p-InP substrate under study was determined by this model [9–14]. Interest in InP as a material for electronic and photonic devices such as junction field effect transistors (JFET) and laser diodes, hydrogen sensing devices, solid-state sensors has increased rapidly over the last few years [2–4, 6, 40–46].

The decrease in the BH at low temperatures leads to nonlinearity in the activation energy $\ln(I_0/T^2)$ versus $1/T$ plot. The nature and origin of the decrease in the BH and increase in the ideality factor with a decrease in temperature and all of the electrical anomalies in the SBDs may be attributed to the presence of Schottky barrier height (SBH) inhomogeneity [6–16, 30–39]. The barrier height is likely a function of the interface atomic structure, and the atomic inhomogeneities at the metal–semiconductor (MS) interface which are caused by grain boundaries, multiple phases, facets, defects, a mixture of different phases, etc [9–17, 31–39]. Additionally, there may be doping inhomogeneity at the MS interface, dopant clustering. Contamination at the MS interface due to undesirable reaction products or particulates is often present at the MS interfaces of diodes prepared by the routine processing methods used in

 © 2008 IOP Publishing Ltd Printed in the UK

the semiconductor electronics industries. These contaminants may act directly to introduce inhomogeneity or they may simply promote inhomogeneity, through the generation of defects [29–37].

Tung and coworkers [38, 39] have modeled imperfect Schottky contacts by assuming lateral variations of the barrier height. They [38, 39] found larger ideality factors and smaller effective barrier heights when they increased the inhomogeneity of barriers. Consequently, two different approaches are adopted by researchers to describe the inhomogeneities [10–13, 38, 39], as mentioned in [9]. One approach assumes a continuous spatial distribution of SBH, and the total current across a Schottky diode is simply calculated by integrating the current determined by the thermionic emission model with an individual barrier height and weighted by using the Gaussian distribution function [10–13]. This approach [12, 13] does not address the lateral length scale of the inhomogeneity, the bias dependence of the SBH, namely, potential pinch-off, as stated in [38, 39]. The other approach [38, 39] assumes that small patches of low SBH are embedded in the uniform SBH area. Using a pinch-off model, the current through a small patch is similar to a diode with an effective SBH and an effective area which are dependent on the patch parameter and the bias voltage.

2. Experimental procedure

The samples have been prepared using cleaned and polished p-InP (as received from the manufacturer) with (1 0 0) orientation and 4–8 $\times$ 10^{17} cm^{-3} carrier concentration given by the manufacturer. We obtained a carrier concentration value of 6.0 $\times$ 10^{17} cm^{-3} from the reverse bias C^{-2}–V characteristics at room temperature. Before making contacts, the n-GaAs wafer was dipped in $5H_2SO_4$ + H_2O_2 + H_2O solution for 1.0 min to remove the surface damage layer and undesirable impurities and then in H_2O + HCl solution and then followed by a rinse in de-ionized water of 18 MΩ. The wafer has been dried with high-purity nitrogen and inserted into the deposition chamber immediately after the etching process. An ohmic contact on the back side of the p-type InP is formed by sequentially evaporating Zn and Au layers on InP in a vacuum-coating unit of 10^{-6} Torr. Then, low resistance ohmic contact was formed by thermal annealing at 350 °C for 3 min in flowing N_2 in a quartz tube furnace. The Schottky contacts have been formed by evaporating Ti as dots with a diameter of about 1 mm on the front surface of the p-InP. The I–V characteristics of the devices were measured using a Keithley 487 picoammeter/voltage source in the temperature range of 20–400 K by means of a temperature controlled cryostat which enables us to make measurements in the temperature range of 20–450 K under dark conditions. The sample temperature was always monitored by using a copper–constantan thermocouple and an auto-tuning temperature controller with sensitivity better than ±0.1 K.

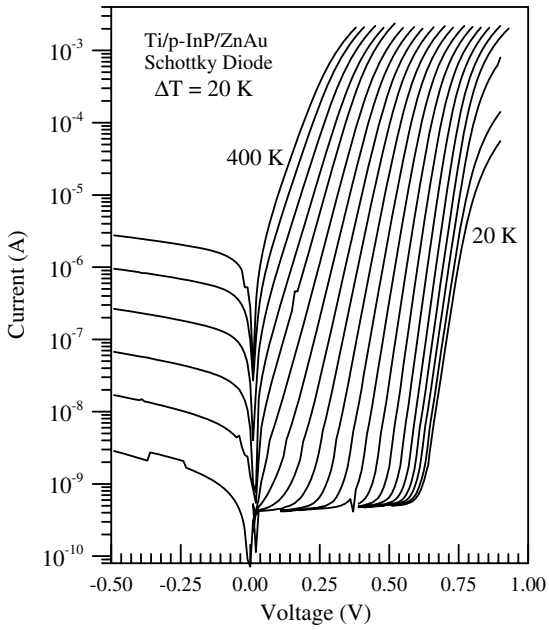

Figure 1. Experimental current–voltage characteristics of a Ti/p-InP/Zn-Au Schottky contact at various temperatures.

3. Results and discussion

3.1. The electrical current–voltage (I–V) measurements

The forward bias current through a uniform metal–semiconductor interface due to thermionic emission (TE) can be expressed as [2]

$$I = I_0 \left[\exp\left(\frac{qV}{nkT}\right) - 1 \right] \tag{1}$$

where I_0 is the saturation current derived from the straight line intercept of $\ln I$ at $V = 0$ and is given by

$$I_0 = A\ A^*\ T^2\ \exp\left(-\frac{q\Phi_{ap}}{kT}\right), \tag{2}$$

Φ_{ap} is the zero bias apparent (experimental) barrier height (BH), q is the electron charge, k is the Boltzmann constant, T is the absolute temperature, V is the forward-bias voltage, A is the effective diode area, A^* is the effective Richardson constant of 60 A cm^{-2} K^{-2} for p-type InP [3, 4]. n in equation (1) is the ideality factor and it is introduced to take into account the deviation of the experimental I–V data from the ideal thermionic model. From equation (1), the ideality factor n can be given as

$$n = \frac{q}{kT}\left(\frac{\mathrm{d}V}{\mathrm{d}\ln I}\right). \tag{3}$$

The I–V measurements of the Ti/p-InP Schottky diode were made in a wide temperature range (20–400 K) with a temperature step of 20 K, and the I–V characteristics of one of the dots are given in figure 1. The experimental values of the barrier height Φ_{ap} (effective barrier height) and the ideality factor n for the device were determined from intercepts and slopes of the forward bias ln$I$ versus V plot at each temperature, respectively, using TE theory, that is, equation (2).

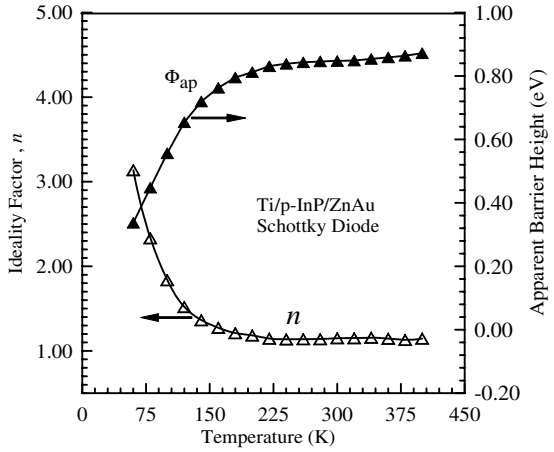

Figure 2. Temperature dependence of the ideality factor (the open triangles) and barrier height (the filled triangles) for the Ti/p-InP/Zn-Au Schottky contact.

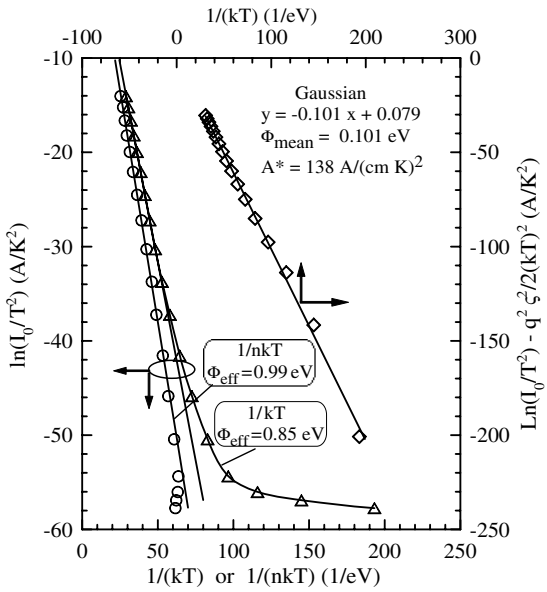

Figure 3. Richardson plot of $\ln(I_0/T^2)$ versus $1/T$ (the open triangles), Richardson plot of $\ln(I_0/T^2)$ versus $1/nT$ (the open circles), and modified Richardson $\ln(I_0/T^2)-q^2\sigma_s^2/2k^2T^2$ versus $1/T$ plot (the open squares) for the Ti/p-InP/Zn-Au Schottky diode according to the Gaussian distributions of barrier heights.

The experimental values of Φ_{ap} and n range from 0.872 eV and 1.145 (at 400 K) to 0.847 eV and 1.150 (at 300 K) to 0.448 eV and 2.63 (at 80 K), respectively. Figure 2 shows the experimental values of n (indicated by open triangles) and Φ_{ap} (indicated by closed triangles) as a function of temperature in the temperature range of 60–400 K. The experimental value of n increased and Φ_{ap} decreased with a decrease in temperature, especially at temperatures below 220 K as can be seen in figure 2. Van Meirhaeghe *et al* [47] obtained a value of about 0.76 eV for evaporated Ti/p-InP Schottky diodes and a value of about 0.96 eV for sputtered Ti/p-InP diodes at room temperature. Van Meirhaeghe *et al* [47] assumed that the barrier height of about 0.76 eV formed on p-type InP by evaporating the contact metal was determined by Fermi level pinning at the interface due to amphoteric defect reactions (involving antisites and vacancies) and consequently the Fermi level is pinned if the concentration of these defects is high enough. They [47] proposed that the value of about 0.96 eV for the sputtered Ti/p-InP diodes is obtained because these defects are passivated by complex formation with H during the sputter metallization process. In the present work, the reason for the fact that the value of 0.847 eV we obtained for the evaporated Ti/p-InP Schottky diodes at 300 K is larger than the value of 0.76 eV given by Meirhaeghe *et al* [47] may be explained by the amphoteric defects with low density on our own p-type InP with respect to that on their p-type InP. Moreover, Van den Berghe *et al* [48] obtained a value of 0.85 eV for the evaporated Ti/p-InP Schottky diodes which is the same as the value of 0.847 eV, we obtained.

Figure 3 (indicated by open triangles) shows a conventional activation energy $\ln(I_0/T^2)$ versus $1/T$ plot according to equation (2). An experimental $\ln(I_0/T^2)$ versus $1/T$ plot shows a significant deviation from linearity at low temperatures. Bowing of the experimental $\ln(I_0/T^2)$ versus $1/T$ curve may be caused by the temperature dependence of the BH and ideality factor due to the existence of the surface inhomogeneities of the p-InP substrate [6–16, 28–39]. As will be discussed below, the deviation in the Richardson plots may be due to the spatially inhomogeneous BHs and potential fluctuations at the interface that consist of low and high barrier areas, that is, the current through the diode will flow preferentially through the lower barriers in the potential distribution [28–39]. A barrier height value of 0.85 eV was obtained from the linear portion of the experimental $\ln(I_0/T^2)$ versus $1/T$ plot. This value corresponds to the value of 0.85 eV at 300 K. The plot indicated by closed triangles in figure 3 shows a conventional activation energy $\ln(I_0/T^2)$ versus $1/n$T which gives a barrier height value of 0.99 eV. The barrier inhomogeneities may occur as a result of inhomogeneities in the interfacial oxide layer composition, non-uniformity of the interfacial charges and interfacial oxide layer thickness [8, 12]. In such cases, the current across the MS contact may greatly be influenced by the presence of the SBH inhomogeneity [6–16, 28–39]. Furthermore, some authors have mentioned that the ideality factor and the *I–V* barrier height (the saturation current) and all functions derived from them can also be explained and connected with the lateral distribution of barrier height due to the local enhancement of electric field which can also yield a local reduction of the barrier height [8, 31, 38, 49]. Thereby, the commonly observed deviation from the classical thermionic emission theory, as will be discussed below, can be explained by a recent model based on the assumption of a spatial fluctuation of the BH at the interface which is related to thermionic emission over a Gaussian BH distribution [10–14].

As stated already by Song *et al* [12] and also by Werner and Güttler [13], the decrease in the barrier height with a decrease in temperature can also be explained by the lateral distribution of BH if the barrier height has a Gaussian distribution of the barrier height values over the Schottky

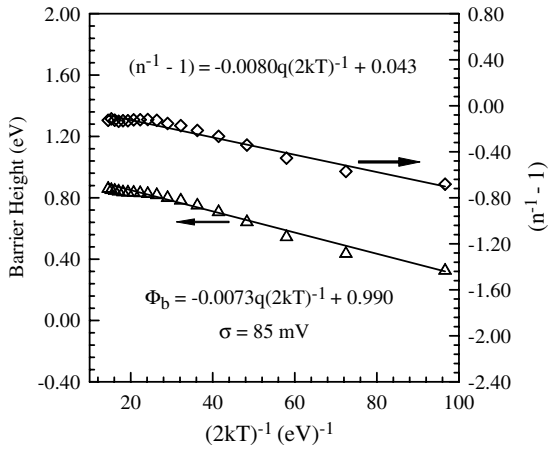

Figure 4. Zero-bias apparent barrier height (the open triangles) and ideality factor (the open squares) versus $1/(2kT)$ curves of the Ti/p-InP/Zn-Au Schottky contact according to the Gaussian distributions of the barrier height.

contact area with the mean barrier height $\bar{\Phi}_b$ and standard deviation σ_s. The standard deviation is a measure of the barrier homogeneity. The Gaussian distribution of the BHs yields the following expression for the BH [10–13]:

$$\Phi_{ap} = \bar{\Phi}_b - \frac{q\sigma_s^2}{2kT}, \tag{4}$$

where Φ_{ap} is the apparent BH measured experimentally. The temperature dependence of σ_s is usually small and can be neglected. The observed variation of ideality factor with temperature in the model is given by [13]

$$\left(\frac{1}{n_{ap}} - 1\right) = -\rho_2 + \frac{q\rho_3}{2kT}, \tag{5}$$

where n_{ap} is the apparent ideality factor (experimental data) and the coefficients ρ_2 and ρ_3 quantify the voltage deformation of the BH distribution. The experimental Φ_{ap} versus $1/T$ and n_{ap} versus $1/T$ plots drawn by means of the experimental data obtained from figure 1 are given in figure 4 for the temperature range of 60–400 K. The linearity of the apparent barrier height (experimental data) or ideality factor versus $1/T$ curves in figure 4 shows that the temperature-dependent experimental data of the Ti/p-InP Schottky contact are in agreement with the recent model which is related to thermionic emission over a Gaussian BH distribution [10–13]. The plot of Φ_{ap} versus $1/T$ (figure 4) should be a straight line with the intercept at the ordinate determining the zero bias mean BH $\bar{\Phi}_{bo}$ and a slope giving the zero bias standard deviation σ_s. The intercept and slope of these straight lines related to Φ_{ap} versus $1/T$ plot have given values of $\bar{\Phi}_{bo}$ and σ_s as 0.99 eV and 85 mV. As mentioned above, the standard deviation is a measure of the barrier homogeneity. The lower value of σ_o corresponds to more homogeneous BH. Clearly, the diode with the best rectifying performance presents the best barrier homogeneity with the lower value of standard deviation. It was seen that the value of $\sigma_o = 0.85$ V is not small compared to the mean value of $\bar{\Phi}_{bo} = 0.99$ eV, and it indicates the presence of the interface inhomogeneities. Nevertheless, this inhomogeneity and potential fluctuation dramatically affect low temperature *I–V* characteristics. It is responsible, in particular, for the curved behavior in the Richardson plot in figure 3 [8–15]. This value of $\bar{\Phi}_{bo} = 0.99$ eV is the same as the value of $\bar{\Phi}_{bo} = 0.99$ eV from the $\ln(I_0/T^2)$ versus $1/nT$ plot (figure 3). Similarly, as can be clearly seen from figure 4 for the temperature range of 60–400 K, the value of ρ_2 obtained from the intercept of the experimental n_{ap} versus $1/T$ plot is –0.043, and the value of ρ_3 from the slope is –0.008 V. The linear behavior of this plot demonstrates that the ideality factor indeed expresses the voltage deformation of the Gaussian distribution of the Schottky BH.

The conventional activation energy $\ln(I_0/T^2)$ versus $1/T$ plot has showed nonlinearity at low temperatures, as indicated above. To explain these discrepancies, according to the Gaussian distribution of the BH, we get

$$\ln\left(\frac{I_0}{T^2}\right) - \left(\frac{q^2\sigma_s^2}{2k^2T^2}\right) = \ln(AA^*) - \frac{q\bar{\Phi}_b}{kT} \tag{6}$$

by considering equations (2) and (4). A modified activation energy plot from this expression is obtained. Using the experimental I_0 data, a modified $\ln(I_0/T^2) - q^2\sigma_s^2/2k^2T^2$ versus $1/T$ plot according to equation (6) should give a straight line with the slope directly yielding the mean $\bar{\Phi}_b$ and the intercept (=ln AA^*) at the ordinate determining A^* for a given diode area A. The $\ln(I_0/T^2) - q^2\sigma_s^2/2k^2T^2$ values were calculated using the value of σ obtained from the Φ_{ap} versus $1/T$ plot (figure 4). Thus, the open squares in figure 3 have given the modified $\ln(I_0/T^2) - q^2\sigma_s^2/2k^2T^2$ versus $1/T$ plots for the value of σ_s. The best linear fitting to these modified experimental data (the open squares) is depicted by the solid line in figure 3 which represents the true activation energy plots in the temperature range of 60–400 K. From this plot has been found a zero bias mean BH$\bar{\Phi}_b$of 1.01 eV. This value is in close agreement with the values of 0.99 eV obtained from the Φ_{ap} versus $1/T$ and $\ln(I_0/T^2)$ versus $1/nT$ plots. The intercept at the ordinate of the modified $\ln(I_0/T^2) - q^2\sigma_s^2/2k^2T^2$ versus $1/T$ plot gives the Richardson constant A^* as 138 A cm^{-2} K^{-2} without using the temperature coefficient of the BHs. The obtained Richardson constant value is about 2.3 times larger than the value of 60 A cm^{-2} K^{-2} known for p-type InP [3, 4].

The T_0 effect, called the temperature-dependence of the BH and ideality factor in Schottky diodes, is also connected either with the lateral inhomogeneity of the barrier height, or with the role of the recombination and tunneling current components [31, 38, 50]. Figure 5 shows a plot of nT versus T reporting the temperature dependence of the ideality factor n; the straight line corresponding to $n = 1$ represents the ideal behavior of a Schottky contact. In this behavior, the straight line fitted to the experimental values for T_0 effect should be parallel to that of the ideal Schottky contact behavior. As can be seen from figure 5, the straight line fitted to the experimental values is parallel to that of the ideal Schottky contact behavior in the temperature range of 180–400 K and it gives a T_0 value of 23.07 K. The plot deviates from thermionic emission (TE) or the ideal Schottky contact behavior below 180 K. As expressed above, this is explainable in terms of the SBH inhomogeneity or of the lateral distribution of the barrier height due to the

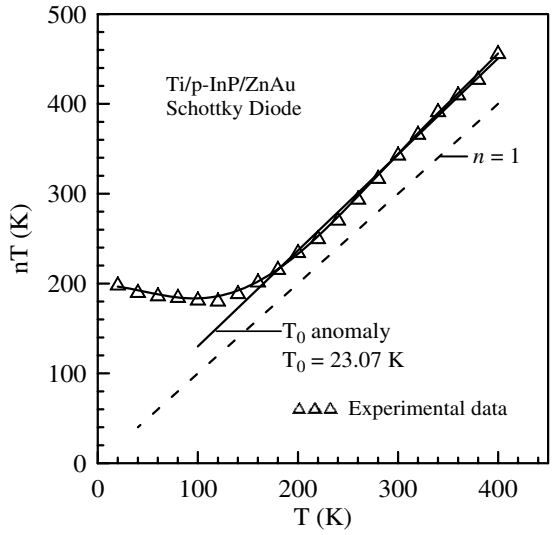

Figure 5. Plot of nT as a function of T showing the T_0 anomaly $n = 1 + T_0/T$. The straight line of the ideal behavior $n = 1$ is also shown.

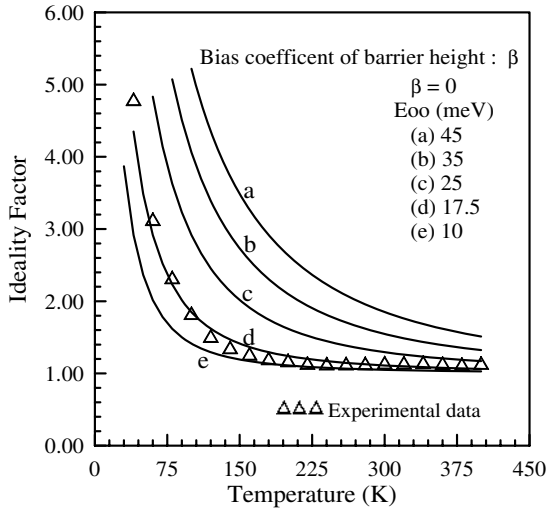

Figure 6. Theoretical temperature dependence of the ideality factor according to equation (10), the bias coefficient of barrier height, $\beta = 0$. The open triangles show the experimental temperature dependence values of ideality factor obtained from the current–voltage characteristics given in figure 1.

local enhancement of electric field which can also yield a local reduction of the barrier height [8, 13, 31, 38, 49].

As mentioned in [8–14], some authors have explained that the ideality factor and the *I–V* barrier height (the saturation current) and all functions derived from them can be explained by means of the Gaussian distribution of the barrier height. It has been shown that these parameters and their functions can also be explained by the dominance of thermionic field emission (TFE) [8, 13, 31, 38, 49–52]. However, one cannot distinguish between the two possible origins on the basis of the *I–V* characteristics alone, that is, the domination of TFE can be connected with the lateral distribution of barrier height because the enhancement of the transmission probability can be due to the local enhancement of electric field which can also yield a local reduction of the barrier height [8, 13, 31, 38, 49–52]. In our case, it may be said that the domination of TFE can be connected with the Gaussian distribution of the barrier height. As indicated above, the similar temperature dependences of ideality factor and apparent barrier height are usually explained by the lateral distribution of barrier height. If the current transport is controlled by the TFE theory due to the local enhancement of electric field which can also yield a local reduction of the barrier height, the relationship between the current and voltage can be expressed by [2, 3]

$$I = I_0 \exp\left(\frac{qV}{E_0}\right) \tag{7}$$

with

$$n_{\text{tun}} = \frac{E_{00}}{kT}\coth\left(\frac{E_{00}}{kT}\right) = \frac{E_0}{kT} \tag{8}$$

where E_{00} is the characteristic tunneling energy that is related to the tunnel effect transmission probability:

$$E_{00} = \frac{h}{4\pi}\left(\frac{N_a}{m^*\varepsilon_s}\right)^{1/2}, \tag{9}$$

where $h = 6.626 \times 10^{-34}$ J s, in the case of the p-type InP with 6.0×10^{17} cm^{-3}, $m^* = 0.64m_o$ and $\varepsilon_s = 12.4\varepsilon_o$, and E_{00} was found to be about 5.0 meV. When considering the bias coefficient of the barrier height, β, equation (8) can be written as [31]

$$n_{\text{tun}} = \frac{E_0}{kT(1-\beta)}. \tag{10}$$

Figure 6 represents the theoretical temperature dependence of ideality factor for the case when the current through Schottky junction is dominated by the TFE. The solid lines in figure 6 were obtained by fitting equation (10) to the experimental temperature dependence values of the ideality factor presented for different values of the characteristic energy E_{00} without considering the bias coefficient of the barrier height, $\beta = 0$. The open triangles in the figure 6 show the temperature dependence values of the ideality factor obtained from the experimental current–voltage characteristics in figure 1. As can be seen from figure 6, the experimental temperature dependence of the ideality factor is in agreement with $E_{oo} = 17.5$ meV in the temperature range of 180–300 K. This value of the characteristic energy E_{00} is 3.5 times larger than the value of 5 meV calculated for the p-type InP. Such a difference between the theoretical and experimental data is usually obtained and expected for Schottky diodes and the case is connected with local enhancement of electric field which can also yield a local reduction of the barrier height [8, 31].

4. Conclusion

It has been seen that the temperature-dependent current–voltage (*I–V*) characteristics of Ti/p-InP SBD obey the Gaussian distribution of BHs. Furthermore, the modified $\ln(I_0/T^2) - q^2\sigma_s^2/2k^2T^2$ versus $1/T$ plot has given $\bar{\Phi}_b$ and A^* as 1.01 eV, and 138 A cm^{-2} K^{-2}, respectively. The Richardson

constant value is about 2.3 times larger than the value of 60 A cm^{-2} K^{-2} known for p-type InP. Furthermore, in the studied temperature range, even although the experimental values of ideality factor are in agreement with the curve (*d*) obtained using the characteristic energy value of 17.5 mV in figure 6, we have stated that the domination of TFE can be connected with the lateral distribution of barrier height because the enhancement of the transmission probability can be due to local enhancement of electric field which can also yield a local reduction of the barrier height.

Acknowledgments

This work was supported by Dicle University (project no:–DÜBAP-07-01-27). The authors wish to thank the Dicle University.

References

[1] Kim D M, Kim D H and Lee S Y 2007 *Solid-State Electron.* **51** 865
[2] Rhoderick E H and Williams R H 1988 *Metal–Semiconductor Contacts* (Oxford: Clarandon Press)
[3] Hökelek E and Robinson G Y 1981 *Solid-State Electron.* **24** 99
[4] Williams R H and Robinson G Y 1985 *Physics and Chemistry of III–V Compound Semiconductor Interfaces* ed C W Wilmsen (New York: Plenum)
[5] Öztas M, Bedir M, Kayalı R and Aksoy F 2006 *Mater. Sci. Eng.* B **131** 94
[6] Cetin H and Ayyildiz E 2005 *Semicond. Sci.Technol.* **20** 625
[7] Gur E Tuzemen S, Kilic B and Coskun C 2007 *J. Phys. Condens. Matt.* **19** 196206
[8] Aydin M E, Yıldırım N and Turut A 2007 *J. Appl. Phys.* **102** 043701
[9] Zhu S, Van Meirhaeghe R L, Detavernier C, Cardon F, Forment S, Ru G P, Qu X P and Li B Z 2000 *Solid-State Electron.* **44** 663
[10] Chand S and Kumar J 1997 *J. Appl. Phys.* **82** 5005
[11] Chand S and Bala S 2005 *Appl. Surf. Sci.* **252** 358
[12] Song Y P, Van Meirhaeghe R L, Laflére W H and Cardon F 1986 *Solid-State Electron.* **29** 633
[13] Werner J H and Güttler H H 1991 *J. Appl. Phys.* **69** 1522
[14] Gümüş A, Türüt A and Yalçın N 2002 *J. Appl. Phys.* **91** 245
[15] Pérez R, Mestres N, Montserrat J, Tournier D and Godignon P 2005 *Phys. Stat. Sol.* (a) **202** 692
[16] Roccaforte F, La Via F, Raineri V, Pierobon R and Zanoni E 2003 *J. Appl. Phys.* **93** 9137
[17] Arehart A R, Moran B, Speck J S, Mishra U K, DenBaars S P and Ringel S A 2006 *J. Appl. Phys.* **100** 023709
[18] Qasrawi A F 2006 *Semicond. Sci. Technol* **21** 794
[19] El-Nahass M M, Zeyada H M, Abd-El-Rahman K F and Darwish A A A 2007 *Sol. Energy Mater. Sol. Cells* **91** 1120
[20] Rouag N, Boussouar L, Toumi S, Ouennoughi Z and Djouadi M A 2007 *Semicond. Sci. Technol.* **22** 369
[21] Kanbur H, Altindal S and Tataroglu A 2005 *Appl. Surf. Sci.* **252** 1732
[22] Pattabi M, Krishnan S, Ganesh and Mathew X 2007 *Solar Energy* **81** 111
[23] Dokme I, Altindal S and Bulbul M M 2006 *Appl. Surf. Sci.* **252** 7749
Dokme I and Altindal S 2006 *Semicond. Sci. Technol.* **21** 1053
[24] Yakuphanoglu F 2007 *Physica* B **389** 306
[25] Kumar S, Katharria Y S, Kumar S and Kanjilal D 2006 *J. Appl. Phys.* **100** 113723
[26] Brovelli F, Rivas B L and Bernede J C 2007 *J. Chilean Chem. Soc.* **52** 1065
[27] Dimitruk N L, Borkovskaya O Y, Dimitruk I N, Mamykin S V, Horvath Z J and Mamontova I B 2002 *Appl. Surf. Sci.* **190** 455
[28] Kim S W, Lee K M, Lee J H and Seo K S 2005 *IEEE Electron Device Lett.* **26** 787
[29] von Wenckstern H, Biehne G, Rahman R A, Hochmuth H, Lorenz M and Grundmann M 2006 *Appl. Phys. Lett.* **88** 092102
[30] Osvald J and Horvath Zs 2004 *Appl. Surf. Sci.* **234** 349
[31] Horváth Zs J 1996 *Solid-State Electron* **39** 176
Ayyildiz E, Cetin H and Horvath Zs J 2005 *Appl. Surface Sci.* **252** 1153
[32] Jones F E, Hafer C D, Wood B P, Danner R G and Lonergan M C 2001 *J. Appl. Phys.* **90** 1001
[33] Im H J, Ding Y, Pelz J P and Choyke W J 2001 *Phys. Rev.* B **64** 075310
[34] Rossi R C and Lewis N S 2001 *J. Phys. Chem.* B **105** 12303
[35] Zhu S, Van Meirhaeghe R L, Forment S, Ru G and Li B 2004 *Solid-State Electron.* **48** 29
[36] Osvald J 1999 *J. Appl. Phys.* **85** 1935
Dobrocka E and Osvald J 1994 *Appl. Phys. Lett.* **65** 575
Osvald J 2006 *Solid-State Electron.* **50** 228
[37] Dogan H, Yıldırım N, Turut A, Biber M, Ayyıldız E and Nuhoglu C 2006 *Semicond. Sci. Technol.* **21** 822
[38] Tung R T 1992 *Phys. Rev. B* **45** 13509
[39] Sullivan J P, Tung R T, Pinto M R and Graham W R 1991 *J. Appl. Phys.* **70** 7403
[40] Perkins J H, OKeefe M F, Miles R E and Snowden C M 1994 *Proc. 6th Int. Conf. on Indium Phosphide and Related Materials (Santa Barbara, CA, 1994)* pp 190–3
[41] Morikita S and Ikoma H 2003 *J. Vac. Sci. Technol.* A **21** 226
[42] Barbariu F, Guillot C, Achard J, Dugay M, Lauren B and Kim D Z 1997 *J. Physique III (France)* **7** 1523
[43] Chen H I and Chou Y I 2004 *Semicond. Sci. Technol.* **19** 39
[44] Korobov V, Leibovitch M and Shapira Y 1993 *J. Appl. Phys.* **74** 3251
[45] Palmer J W, Anderson W A and Cartwright A 1997 *IEEE Photonics Technol. Lett.* **9** 1385
[46] Newman N, Van Schilfgaarde M and Spicer W E 1987 *Phys. Rev.* B **35** 6298
[47] Van Meirhaeghe R L, Laflere W H and Cardon F 1994 *J. Appl. Phys* **76** 403
[48] Van den Berghe L M D, Van Meirhaeghe R L, Laflere W H and Cardon F 1990 *Solid-State Electron.* **33** 79
[49] Duman S, Gurbulak B and Turut A 2007 *Appl. Surf. Sci.* **253** 3899
[50] Hardikar S, Hudait M K, Modak P, Krupanidhi S B and Padha N 1999 *Appl. Phys.* A **68** 49
[51] Horvath Zs J 1988 *J. Appl. Phys.* **64** 6780
[52] Horvath Zs J, Rakovics V, Szentpali B, Puspoki S and Zdansky K 2003 *Vacuum* **71** 113